LITERATURE CITED

1. Jones, A. L., *Ind. Eng. Chem.*, **47**, 212 (1955).
2. ———, *Petrol. Process.*, **6**, 132 (1951).
3. ———, and R. W. Foreman, *Ind. Eng. Chem.*, **44**, 2249 (1952).
4. Sellbach, C. W., and R. W. Quackenbush, *J. Am. Oil Chemists' Soc.*, **34**, 603 (1957).
5. ———, *Ind. Eng. Chem.*, **50**, 353 (1958).
6. Anon., *Chem. Eng. News*, **39**, 69 (April 3, 1961).
7. Washall, T. A., and F. W. Melpolder, *Ind. Eng. Chem., Process Design Dev.*, **1**, 26 (1962).
8. Debye, Peter, and A. M. Bueche, "High Polymer Physics," H. A. Robinson, ed., p. 497, Chemical Publishing, Brooklyn, New York (1948).
9. Sullivan, L. J., T. C., Ruppel, and C. B. Willingham, *Ind. Eng. Chem.*, **49**, 110 (1957).
10. Lorenz, Maurice, and A. H. Emery, Jr., *Chem. Eng. Sci.*, **11**, 16 (1959).
11. Lorenz, Maurice, Ph.D. thesis, Purdue Univ., Lafayette, Ind. (1960).
12. Crownover, C. F., and J. E. Powers, *A.I.Ch.E. Journal*, **8**, 166 (1962).
13. Powers, J. E., and C. R. Wilke, *ibid.*, **3**, 213 (1957).

Manuscript received December 10, 1962; revision received April 8, 1963; paper accepted April 10, 1963. Paper presented at A.I.Ch.E. Buffalo meeting.

The Interrelation of Geometry, Orientation, and Acceleration in the Peak Heat Flux Problem

C. P. COSTELLO and J. M. ADAMS

University of Washington, Seattle, Washington

Boiling heat transfer is widely employed in high-performance systems owing to the fact that extremely high energy transfer rates per unit area (that is, heat fluxes) may be obtained with relatively low surface to fluid temperature differences. At a certain heat flux, a vapor film is able to stabilize on the heater surface, partially insulating it and causing it to overheat. The unit energy transfer rate at which this condition occurs will be called the *peak heat flux* in this paper.

Certain analytic and semianalytic correlations [that is, (*1, 2, 3*)] have been proposed to enable prediction of the peak heat flux with varying degrees of success. More extensive study of the problem is required to ascertain the correct picture of the physical situation at the peak heat flux condition.

Studies of the effects of high accelerations on the peak heat flux are desirable from at least two standpoints:

1. Certain systems employ boiling heat transfer in various acceleration fields.
2. Most important, when accelerations are imposed on systems there is a means of appraising the realism of physical models which have been used to devise various peak heat flux correlations.

For these reasons, some attention has been given to studies of the effects of acceleration on peak heat flux. Gambill and his co-workers, (*4, 5*) studied spiral flows of water in channels where centripetal accelerations were obtained owing to the path of the fluid. Gambill and Greene (*4*) indicated that the peak heat flux, $(q/A)_p$, appeared to be related to the acceleration divided by local gravitational acceleration, (a/g), as follows:

$$(q/A)_p \propto (a/g)^{0.43-0.48} \qquad (1)$$

But since the fluid was below its saturation temperature and flowing at high velocity, Gambill and Greene were reluctant to ascribe all of the increases in $(q/A)_p$ to acceleration effects.

To eliminate these confounding factors, Costello and Adams (*6*) ran pool boiling tests wherein the pool was rotated to produce accelerations up to $a/g = 40$. For values of a/g up to 10 the data showed

$$(q/A)_p \propto (a/g)^{0.15} \qquad (2)$$

while for $a/g > 10$

$$(q/A)_p \propto (a/g)^{0.25} \qquad (3)$$

Equation (3) shows the behavior that the analytic correlations of Zuber et al. (*2*), Borishanskii (*3*), and others have predicted. No correlations predict the behavior of Equation (2), however.

Choi (*7*) imposed magnetically produced accelerations on a system in which Freon-113 was pool boiled. When he plotted his data in terms of an equivalent acceleration, they bore striking similarity to those of Costello and Adams (*6*) in that for lower accelerations the data behaved according to Equation (2) while at high accelerations Equation (3) characterized the data. Ivey (*9*) conducted tests using stainless steel cylinders 0.048-in. O.D. and 1.25 in. long. These were rotated in a centrifuge and Ivey found that Equation (2) held over the range $1 \leq a/g \leq 160$. However, it was necessary to correct for substantial pressure buildups and subcoolings in the centrifuge employed by Ivey, and this required the use of techniques which may not be valid for $a/g > 1$. At any rate, few data were taken in the range $1 \leq a/g \leq 10$.

Usiskin and Siegel (*8*) obtained some data on the effects of accelerations less than that of normal gravity $(a/g < 1)$ by means of drop tests. Since the existence of steady state was uncertain, the data are questionable to some extent, but they appear to behave in the manner

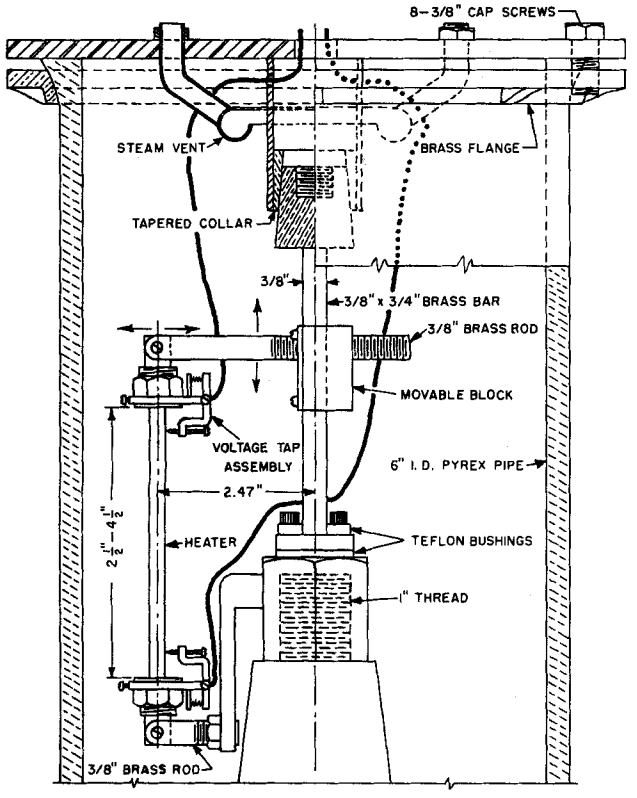

Fig. 1. Experimental apparatus.

predicted by Equation (2). The results of Usiskin and Siegel will be discussed further below. Works are also available on the effects of acceleration on the nucleate boiling heat transfer coefficient. Merte and Clark (*10*), Slember (*11*), Costello and Tuthill (*12*), and Costello and Adams (*6*) have published on this subject, and certain of their results have been useful in the formulation of the correlation presented in this paper.

APPARATUS*

Figure 1 illustrates the apparatus and shows the pertinent dimensions. Heaters of various shapes (cylinders, semicylinders, and flat plates) were mounted with their axes vertical between the incoming power loads. Thus, by rotating the container about its vertical axis, a centripetal acceleration was produced which acted normally to the heater axis. Although local gravity acted upward, its effect was small compared to that of centripetal acceleration for the majority of tests. The fluid boiled was distilled water which had been deaerated by boiling prior to the tests. The fluid and heater were rotated together as a solid body.†

The centripetal acceleration was determined from measurements of the rate of rotation of the Pyrex pipe shown in Figure 1; the measurements were made with a calibrated tachometer.

Direct current was supplied to the test section from a full wave rectifier. Amperage was determined by measuring the voltage drop across a calibrated shunt. Each heater contained a reduced section in the middle of its vertical extent across which minute voltage taps were placed. The voltage taps rotated with the equipment and provided a reading of the voltage across the very section where peak heat flux occurred. The facts that peak heat fluxes were experienced in the reduced portion of the heater elements, and that the reduced portions were located centrally with respect to the heater length, precluded end effects. The lengths of the reduced sections of the heaters were chosen to be in excess of 2 in. and of sufficient section so that no size effects would be present, according to Bernath (*13*). Flat plate heaters were about 5/16 in. wide.

The voltage drop across each heater was determined with a potentiometer in conjunction with a calibrated resistance circuit. (See Figure 2.) The high resistance (10^5 ohms) prevented any large currents from flowing in the circuit parallel to the heater in Figure 2 so that there would be only negligible voltage drops across the brushes used to transmit the voltage measurement. This arrangement permitted highly accurate and sensitive voltage measurements.

Since the only data taken were voltage, amperage, and container angular velocity, these variables could be carefully monitored on highly precise instruments. The uncertainty estimates in Table 1 verify the accuracy of the arrangement; the only appreciable uncertainty in peak heat flux was due to the necessity of changing the power level by finite increments when searching for the peak flux. The uncertainty arising from this source is included in the estimate given in Table 1.

The peak heat flux was detected in the following manner. The pool was brought to saturation and boiled vigorously for some 15 min. The rotational velocity was set and maintained. Power to the heater was slowly increased until the heat flux was about 10% below the anticipated peak flux. Power was then increased so that the increments in heat flux were about $10{,}000 \frac{\text{B.t.u.}}{\text{hr. sq.ft.}}$. After each increment, the setting was held for 1 to 2 min., and then the power was increased again.

When the peak heat flux was reached, the voltmeter and ammeter readings changed in a distinctive manner and the power was shut off. Time was allowed for the film on the heater to dissipate, and another test was begun with all steps repeated except the 15 min. boiling period.

All heaters used were of graphite of the purest type available. It was found that if the power were shut off immediately upon the attainment of peak heat flux, the heaters could be used repeatedly with no aging effect. That this was so was verified frequently for each heater by repeating peak heat flux determinations at a reference condition (zero rev./min. of the container).

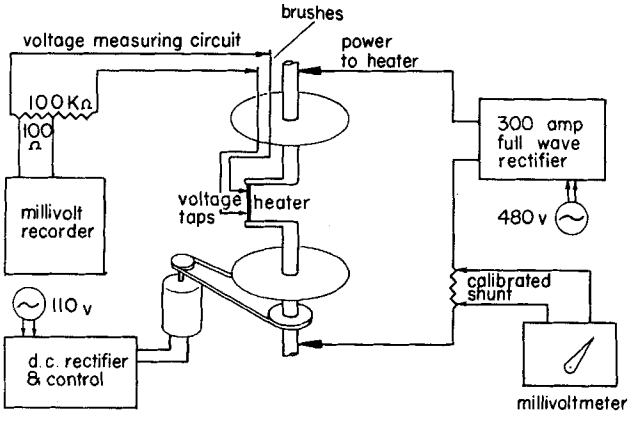

Fig. 2. Power and instrumentation diagram.

TABLE 1. EXPERIMENTAL UNCERTAINTIES IN THE VARIABLES

Presented values	95% confidence interval
$(q/A)_{peak} = 395{,}000$	±11,200
$(q/A)_{peak} = 1{,}000{,}000$	±25,300
$(a/g) = 2.4$	±.628*
$(a/g) = 74.9$	±3.59
$\sigma = 27.55$ to 71.45	±3.1†

* Only essential details are given here. A more complete description is given in references 6 and *14*.

† For tests at $a/g = 1$, the heater was mounted horizontally in a separate pool to obtain closer correspondence with tests at $a/g > 1$.

* Values of uncertainty in a/g presented are those relative to average values of a/g. They do not account for the small variation in a/g across the heater surface.

† Joint estimate of uncertainty in surface tension based on all measurements.

Asbestos and Bakelite were used to insulate portions of the heaters during tests of semicylinders and flat plates. The insulation devised was extremely effective, and no heat leakage had to be accounted for since it was estimated to be only about 1% of the peak heat flux, using assumptions which would maximize the leakage (*14*).

Fluid level was maintained by periodically adding degassed boiling liquid to the container from a preheater. It is estimated that the liquid level was maintained at least 1 in. above the heater and was no more than 1.75 in. above the heater during all tests. The center of the apparatus was well vented so that the pressure at the test section was essentially atmospheric. Steam was allowed to issue through special vents, and this provided evidence of the saturation of the pool.

VALIDITY OF THE METHOD

The use of a centrifuge affords a convenient means of studying the effects of acceleration on boiling, but the following confounding effects are present, and it must be verified that they do not become appreciable.

Pressure Buildup Due to Centrifugal Action

Due to rotation, the pressure at the heater location exceeded that at the free surface by a maximum of 3.5 lb./sq.in. Of itself, this is not too significant since it would only amount to a maximum increase of 10% in the heat flux owing to variation in property values due to pressure variations. [The equation of Zuber et al. (2) was used in this evaluation.] At most accelerations, the peak heat flux values were unaffected by pressure increases.

Subcooling

The saturation temperature at the free surface was below that at the heater location by a maximum of 9 deg. owing to pressure increase due to rotation. However, the liquid migrates relatively slowly toward the heater, and it is warmed to saturation at the heater location by the countercurrent flow of vapor. The situation is complex, but the authors have ascertained experimentally that no subcooling effects are present at the heater. This was accomplished by actual measurements of pool temperatures, by maintaining the fluid at various levels above the heater (thus, markedly altering the potential subcooling) without noting any effect on the peak heat flux, and by running with heaters located at different radii of rotation (*6*) (thus, again markedly altering the potential subcooling) with no effect on peak heat flux.

Coriolis Acceleration

The supplementary or Coriolis acceleration on the vapor as it moves from the heater is given by

$$a_s = 2U\omega \tag{4}$$

where U is the velocity with which the vapor moves toward the center of the container and ω is the angular velocity. [See for example, (*15*).] The values of a_s can be very large, in the order of 100 times the centripetal acceleration for some U velocities which have been observed photographically in tests at the University of Washington, Seattle, Washington (*16*). However, tests reported below as well as those cited in reference 6 have conclusively shown that Coriolis accelerations do not effect the peak heat flux. This will be discussed in another section on results.

Variation of Acceleration With Radial Location

As bubbles leave the heater and move toward the center of the container, they experience a variable acceleration field rather than a constant one. Since the acceleration equals $\omega^2 z$, where z is the radial distance, one obtains

$$\frac{da}{dz} = \omega^2 \tag{5}$$

For tests with different radial locations of the heater element, different values of ω must be maintained to obtain the same value of acceleration. Since this is so, the rate of change of acceleration with radius must change as well, as Equation (5) shows. Yet tests made with heaters at various radial locations (with as much as 60% difference in radii) have failed to show any significant differences in the data. It must be concluded that there are no appreciable effects owing to the variable acceleration field.

Variation of Pressure With Radius

Since pressure P varies with radius z as follows

$$\frac{dP}{dz} = \rho_l \frac{\omega^2 z}{g_c} \tag{6}$$

the imposition of an acceleration field necessarily results in a variation of pressure with radius. (Here ρ_l is liquid density, g_c a constant of proportionality.) However, the following facts indicate that the variation of pressure with radius exerts no significant effect.

1. A normalization of the Navier-Stokes equation (see Appendix) shows that groups arising from the dP/dz term are orders of magnitude smaller than those arising from buoyancy, inertia, and capillary effects.

The present data compare well with data obtained from devices (references 7, 8) with which no appreciable dP/dz effects occur.

3. In any tests of boiling in a pool, pressure varies with distance from heater owing to the variation of pressure with depth of fluid. This effect is always considered to be negligible in pool boiling tests. In the present tests, the rate at which pressure P varies with location increases as acceleration ($\omega^2 z$) increases, but buoyancy and inertial forces also increase directly with acceleration. Hence, if the effects of the variation of pressure with depth are negligible in ordinary pool boiling, they are probably negligible in a centrifuge.

Secondary Flows

The existence of the pressure gradient, dP/dz, could have led to secondary flows which would be undesirable since the tests were to be of pool boiling behavior. For example, with a flat plate heater, insulated on all sides except that which faces the axis of rotation, bubbles move toward the axis of rotation owing to buoyancy forces. The pressure gradient, dP/dz, would tend to force liquid to the heater face from locations at greater radii than that of the heater surface. Such a tendency exists in all pool boiling tests, but the effect is augmented here owing to the higher values of dP/dz.

There is indirect evidence that such effects are negligible. Agreement of the present data with references 7 and 8, where no such secondary flows exist, exemplifies such evidence. Also, as described in the section on results, flat plate heaters were oriented in various manners with respect to the axis of rotation, and the variation of the orientation should have led to different effects of secondary flow. No such variations were noted.

Direct evidence that secondary flows were unimportant was obtained as follows. A flat plate heater was fitted with large baffles on its sides so that liquid could not reach the surface from locations at greater radii. The baffles extended for 1 in. from each edge of the 5/16-in. wide flat plate heater and thus completely blocked the path of secondary flows. Yet, except for normal scatter, no difference could be seen in the $(q/A)_p$ vs. acceleration data obtained from the heater with baffles as compared to heaters without baffles. This provided direct evidence that no effects of secondary flows were present.

The authors can only conclude after weighing the mass of experimental evidence that the centrifugal acceleration

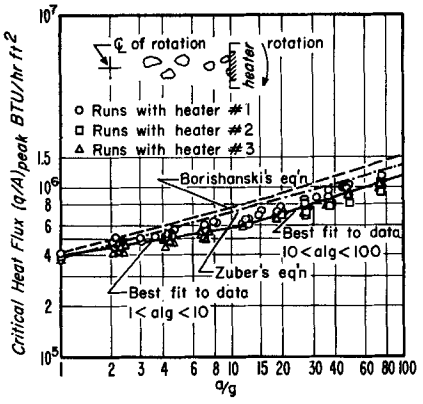

Fig. 3. Peak or critical heat flux vs. acceleration for three flat plate graphite heaters in distilled water. Insulated on all faces except that facing axis of rotation. Equations (7) [Zuber, (2)] and (8) [Borishanskii, (3)] are shown for comparison.

is the only direct cause of the behavior presented in the section on results.

DATA REDUCTION AND AVERAGING

Measurement of voltage, amperage, and total exposed surface area were used to calculate the peak heat flux $(q/A)_p$. The data were programmed for an IBM-709 computer so that the heat flux and total acceleration would be calculated. The local gravitational and centripetal accelerations were combined vectorially to obtain the total acceleration as multiples of the local acceleration of gravity, a/g.

A least squares fit IBM program was used to determine best values of $(q/A)_p$ from the many values taken at each acceleration. The standard deviation at each point was also calculated. The computer also was used to determine the slopes of curves on $(q/A)_p$ vs. a/g coordinates, with the assumption that $(q/A)_p$ was proportional to a/g raised to a constant exponent in various ranges of a/g. The results, as they pertain to the figures presented in this paper, are shown in Table 2. At least four (and often many more) peak heat flux data points were taken at each value of a/g for each geometry and orientation employed. At least two different heaters were used for each geometry and orientation to eliminate any surface effects.*

* Tests were also made in which the fluid surface tension was altered. A minimum of four data points were taken at each value of a/g for each value of surface tension employed.

TABLE 2. LEAST SQUARES FIT OF DATA

Figure	Slope of curve with 95% confidence interval $1.0 \leq a/g \leq 10.0$	Slope of curve with 95% confidence interval $10 \leq a/g \leq 100$	Average deviation of individual measurements from straight line
3	0.156 ± 0.043	0.308 ± 0.031	5.2%
4	0.198 ± 0.031	0.270 ± 0.020	3.6%
6*a*	0.156 ± 0.043	0.308 ± 0.031	5.2%
b	0.148 ± 0.046	0.329 ± 0.022	4.4%
c	0.157 ± 0.047	0.309 ± 0.017	3.3%
d	0.155 ± 0.041	0.284 ± 0.018	3.7%
e	−0.025 ± 0.013	−0.100 ± 0.034	4.7%
7*a*	0.156 ± 0.043	0.308 ± 0.031	5.2%
b	0.184 ± 0.047	0.340 ± 0.016	2.9%
c	0.193 ± 0.068	0.355 ± 0.016	3.2%
f	0.197 ± 0.029	0.424 ± 0.037	7.1%

RESULTS

Flat Plates

Figure 3 shows a typical set of data for a flat plate facing toward the axis of rotation and insulated on all other sides.

The equations of Zuber et al. (2)

$$(q/A)_p \approx 0.131\,\lambda\rho_v\left[\frac{\sigma g_c g(\rho_l-\rho_v)}{\rho_v^2}\right]^{1/4} \tag{7}$$

and of Borishanskii (3)

$$(q/A)_p = \lambda\rho_v^{1/2}\left[\sigma g g_c(\rho_l-\rho_v)\right]^{1/4}\left\{0.13+4\left[\frac{\mu_l^2}{\rho_l g_c}\left(\frac{g(\rho_l-\rho_v)}{\sigma^3 g_c}\right)^{1/2}\right]^{0.4}\right\} \tag{8}$$

are shown on Figure 3 for comparison.

In a calculation of values from Equations (7) and (8), the variations of property values owing to pressure buildup due to rotation have been included. The most substantial variation is in ρ_v, and the variation tends to make the curves steeper on $(q/A)_p$ vs. a/g coordinates. (The effect is only noteworthy for $a/g > 50$.) In fact, when the effects of density variation are included, the slopes of Equations (7) and (8) show

$$(q/A)_p \propto (a/g)^{0.3} \tag{9}$$

at high values of a/g. Although this is in good agreement with the experimental values for $a/g > 10$ (Table 2), the equations do not predict the system behavior in the range $1 \leq a/g \leq 10$. In this range, as Table 2 shows, Equation (2) is a better fit to the data.

Although Chang (1) has proposed a reasonable physical model for the peak heat flux problem, his equation for peak heat flux in a saturated pool contains parameters which the authors were unable to evaluate for the present tests.

It has been mentioned that the term "flat plates" suggests larger heaters than the narrow strips used in the present tests and also that the small strips may be effected differently than larger heaters. However, in the next section, data on cylinders with diameters ranging from ⅛ in. to 5/16 in. will be seen to agree extremely well. Moreover, bubble departure sizes become quite small at high a/g; at $a/g = 40$, bubbles were commonly 0.02 in. at departure. (These would later coalesce into larger vapor slugs which were larger by orders of magnitude.) Thus on a heater 5/16 in. wide, there is room for several adjacent rows of bubbles to grow. These facts would suggest that there may not be substantial size effects.

Cylinders

Cylinders of 1/8, 3/16, 1/4, and 5/16 in. diam. were tested to see if a size effect on the peak heat flux might be present as was suggested earlier (6). Figure 4 shows the results of the tests; the points shown are averages of four points of more for each size heater, and the scatter from these average values was extremely small.

The data of Usiskin and Siegel (8), obtained from drop tests with a small platinum wire, are shown compared to data from the present tests on Figure 4. It is seen from the curve and from Table 2 that Equation (2) fits the data of the present test ($1 \leq a/g \leq 10$) and the data of Usiskin and Siegel ($a/g < 1$) quite well.

The data for all cylinders are in such excellent agreement that the exponents presented in Table 2 for Figure 4 only would have to be varied by plus or minus 5% to include 90% of all data points for all cylinder sizes. It appears that no substantial effect of cylinder size exists in the range of variables of the present test.

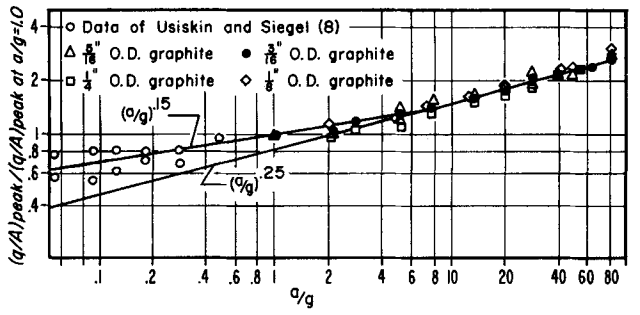

Fig. 4. Peak or burnout heat flux vs. acceleration for cylindrical graphite heaters in distilled water. Data of Usiskin and Siegel (8) shown for comparison. Ordinate is ratio of peak heat flux to peak flux at a/g = 1. Peak heat flux at a/g = 1 was 380,000 B.t.u./hr. sq. ft. in present tests.

Semicylinders

It was noted in a photographic study that the peak heat flux always occurs on that half of a cylindrical heater from which the bubbles detach, never on the half against which the bubbles are held by buoyancy forces. To investigate this phenomenon further, semicylindrical heaters were constructed and tested (*16*).

Runs were made with the semicylindrical heater facing in the direction of the acceleration vector, and other tests were made with the active portion of the heater facing away from the direction of acceleration. The results are shown in Figure 5. At higher accelerations the effects of orientation are seen to be most pronounced. For $a/g > 10$ Equation (3) holds for the semicylinder facing inward (in the direction of the acceleration vector), while for the semicylinder facing outward (away from the direction of the centripetal acceleration)

$$(q/A)_p \propto (a/g)^{0.38} \qquad (10)$$

As stated above, it was noted that film boiling started on the half of the cylindrical heater from which the bubbles detach, while the half against which bubbles were momentarily held by buoyancy forces was still in nucleate boiling. Also, a wave of vapor originated from the bottom of the heater and swept around toward the detaching side. Such a wave invariably came from those portions of the heater against which vapor was momentarily held by buoyancy forces; a wave never formed on the detaching side of the heater. This is thought to account for the differences between configurations A and B in Figure 5 as will be discussed below.

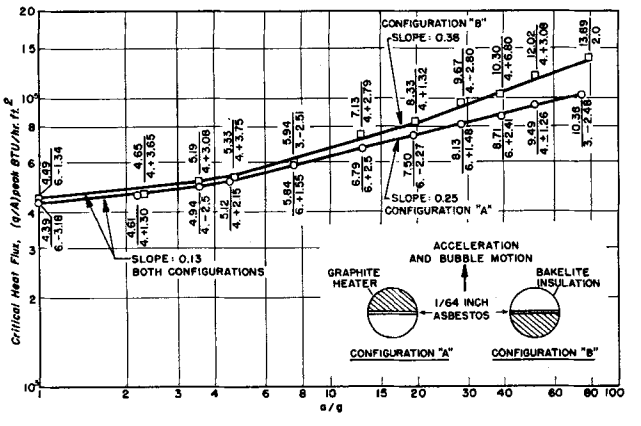

Fig. 5. Peak heat flux vs. acceleration for two orientations of semicylinders in distilled water. Numbers near data points =

$$\frac{\text{Average peak flux}}{\text{No. of tests. Maximum deviation from average}}$$

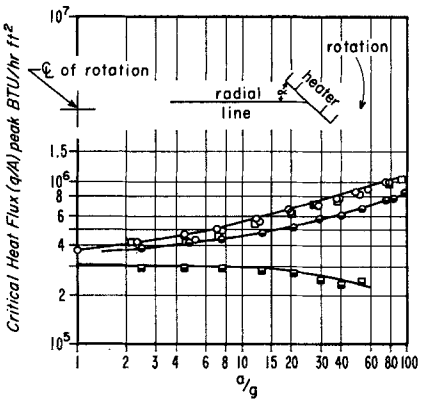

Fig. 6. Peak heat flux vs. acceleration, a/g, for flat plate heaters in distilled water. Heaters oriented in various manners with respect to acceleration vector which is essentially radial.

○ α = 90 deg.
○ α = 45 deg.
□ α = 0 deg.
half solid circle α = 315 deg.
half solid square α = 270 deg.

Checks on Coriolis Acceleration and Flat Plate Orientation

Flat plate heaters were tested in various orientations with respect to the acceleration vector by changing angle α, Figure 6, through 360 deg. by increments of 45 deg. Figure 6 shows some of the results.

Coriolis acceleration vectors are directed normally with respect to the relative velocity of the bubbles. The relative velocity vector is toward the center of the container. Thus, in the case of a flat plate facing toward the center (α = 90 deg., Figure 6), the Coriolis acceleration vector is across the face of the heater. If the plate is facing the direction of rotation of the Pyrex container (α = 0 deg.), the Coriolis acceleration is normally away from the surface. If the surface faces the direction of rotation (α = 180 deg.), the Coriolis acceleration is normally toward the surface. At vapor velocities observed from motion pictures, the Coriolis or supplementary accelerations, a_s, have been evaluated at over 100 times local gravitational acceleration. Yet there was no difference in the behavior of strips with α = 0 as compared to those with α = 180 deg. In fact it was found that Coriolis accelerations could be oriented in any manner with respect to the surface without altering $(q/A)_p$. Since this is so, data from only a few orientations are presented in Figure 6. Complete tabulations and graphs of the data obtained are shown in reference *14*.

Motion picture studies (*16*) as well as consideration of the meaning of Coriolis acceleration* have shown that high values of a_s do not result in high liquid-to-vapor velocities in the direction of a_s. Some researchers maintain that only the relative velocity of vapor with respect to liquid is significant in determining the peak heat flux. This may explain the insensitivity of the system to Coriolis effects. Coriolis accelerations are not incorporated into the reported values of a/g since they are not significant.

Figure 6 shows that to arrange the heater so that the centripetal acceleration is normally away from the heat transfer surface, athwart the surface, or at 45 deg. to the surface makes little difference in the peak heat flux behavior. This result lends some weight to hydrodynamic instability theories which maintain that the breakdown of

* That is, a_s is an absolute acceleration (with respect to a stationary observer) but does not indicate that motion exists between the liquid and vapor phases.

nucleate boiling occurs in the liquid and vapor next to the surface and that the peak heat flux should, therefore, be only slightly sensitive to surface orientation. Flat plate heaters toward which the acceleration vectors are directed (wholly or in part) are seen to suffer reductions in $(q/A)_p$ because buoyancy forces hold bubbles against these surfaces until a film of vapor can stabilize. (Although in the present tests the bubbles are still being removed by local gravity.) This was not the case for cylinders on which the surface curvature facilitated the escape of vapor (see Figure 5).

Surface Tension Tests

A wetting agent was added to the distilled water to reduce surface tensions and thereby to permit the study of the effect of this variable. A maximum weight of 0.1% for the wetting agent was used. Samples of fluid containing the additive were taken to measure the latent heat of vaporization, liquid density, and rate of change of saturation temperature with pressure. The latter was used with the Clapeyron relation to evaluate the vapor density. It was found that none of these variables were altered by as much as 1% from the values for pure water. Since these variables plus the surface tension are the only ones which affect the peak heat flux according to most hydrodynamic instability formulations, it appears that the surface tension is the only significant variable which was changed. Values of the surface tension were measured with a ring tensiometer.

The results of the tests are shown in Figure 7 and Table 2 where it is seen that the slopes of $(q/A)_p$ vs. a/g are increased above those noted for pure water (σ = 71.5 dynes/cm.). The increase is slight in the range $1 \leq a/g \leq 10$ but quite pronounced thereafter. The tendency increases with the lowering of surface tension although there is some scatter. With σ = 32. dynes/cm. (45% of that for pure water) and with $a/g > 10$, the slope given by the IBM-709 program was

$$(q/A)_p \propto (a/g)^{0.42} \qquad (11)$$

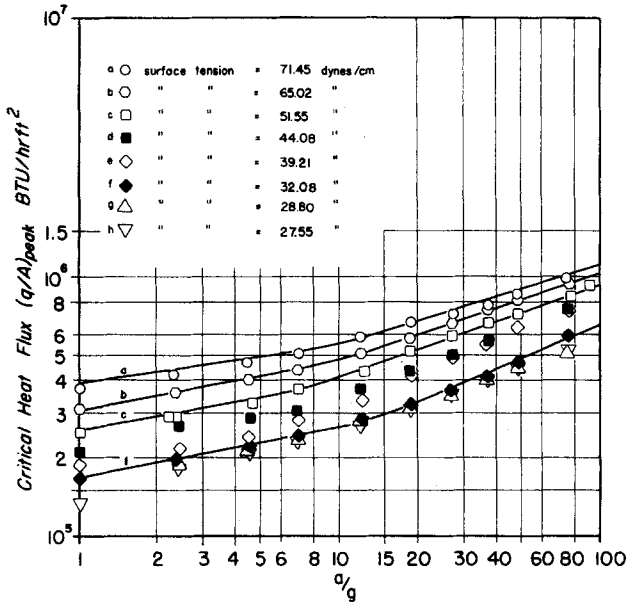

Fig. 7. Peak heat flux vs. acceleration with fluid surface tension as parameter. (All surface tensions evaluated at 25°C but rate of change of σ with temperature was found to be the same with all fluids.) Other fluid properties are those of distilled water within 1%. Flat plate graphite heater facing axis of rotation (α = 90 deg.). Topmost curve for distilled water. (Curves are not drawn through all sets of points to avoid crowding of figure.)

A cross-plot of the data shown in Figure 7 shows that $(q/A)_p$ is nearly proportional to σ at lower values of a/g but is changed by σ to a lesser degree at higher accelerations. Equations based on purely hydrodynamic grounds predict that $(q/A)_p$ will be proportional to σ to the one-fourth power and do not account for the experimentally observed fact that with lower surface tensions $(q/A)_p$ increases more substantially with a/g.

Although Figure 7 was based on numerous and reproducible data, the behavior was so markedly different than that predicted by analytic correlations that a further check was made. Horizontal cylinders, of various materials, ⅛-in. O.D. and 3.75 in. long were tested in clean beakers with both distilled water (σ = 71.5 dynes/cm.) and distilled water with wetting agent (σ = 35 dynes/cm.)

It was found that with stainless steel heaters $(q/A)_p$ varied with σ to the 0.30 power while with a previously unused graphite heater $(q/A)_p$ was proportional to $\sigma^{0.55}$. As noted above, graphite heaters roughened by previous use showed an even stronger dependency on surface tension.

This indicates that forces between the surface and the vapor are significant as Chang (*1*) has stated. It also indicates that surface effects of a nonhydrodynamic nature are important although hydrodynamic theories may be generally used to predict the effects of most system variables.

DIMENSIONLESS NUMBERS THAT CHARACTERIZE THE ACCELERATION EFFECTS

Figure 3 shows a comparison of experimental data with the results of Equations (7) and (8). When the equations were plotted, all property variations owing to the pressure buildup due to centripetal action were accounted for, but the equations are still not consistent with the data. The constants in Equation (8) were altered to see if the dimensionless groups derived by Borishanskii (*3*) were adequate to describe the data, but the effort was unsuccessful.

Studies of motion pictures (*16*) reveal that the imposition of accelerations on a pool boiling system results in less crowded heater; that is, bubble coalescence is reduced and bubbles leave the surface singly or after combination with a few of their neighbors. The data behave in a different manner under these circumstances than when waves of vapor are formed. This is verified when the two curves in Figure 5 are contrasted for high values of a/g. Curve A represents the case in which small groups of bubbles or individual bubbles leave the heater. Curve B shows the behavior characteristic of surfaces on which the waves of vapor form owing to the reorientation of the acceleration vector with respect to the heater.

For the reasons cited above, it seems reasonable to include the geometry of the vapor bubbles or jets in any correlation of the present data. To accomplish this, an order of magnitude analysis was carried out by normalizing the Navier-Stokes equations describing the flow of a bubble or a vapor jet. (The analysis is presented in the Appendix.) It was shown that at least three groups are of significant magnitude in determining the instability of the vapor, that the best way to correlate the data is to arrange these groups as shown below in Equation (12), and that in terms of the dictates of approximation theory the groups should appear as shown in Equation (12):

$$\frac{D\rho_v U_m}{\mu} \propto \frac{D^2(\rho_l - \rho_v)\, g(a/g)}{U_m \mu} \left[C_1 + C_2 \frac{(\sigma g_c)}{U_m \mu} \right] \qquad (12)$$

The group on the left is the vapor Reynolds number which is proportional to destabilizing inertial forces. The

group before the brackets on the right is the Reynolds over the Froude number which is proportional to the stabilizing gravitational force, and the second term in the bracket is the ratio of Reynolds to Weber number which is proportional to the stabilizing cohesive force. As stated in the Appendix, Equation (12) is not complete; other property values would enter through careful consideration of boundary equations for the Navier-Stokes equations. It is felt that all influences of a/g are contained in Equation (12), however, and that the equation contains all forces which might enter the hydrodynamic analysis (viscous, inertial, buoyancy, and capillary).

U_m is regarded as proportional to the peak heat flux as follows:

$$(q/A)_p = \lambda W_v \tag{13}$$

Where λ is the latent heat of vaporization, W_v is the mass flow rate of vapor per unit area. It is also assumed

$$W_v \propto \rho_v U_m \tag{14}$$

so that

$$(q/A)_p \propto \lambda U_m \rho_v \tag{15}$$

and when Equations (12) and (15) are combined, one obtains

$$(q/A)_p \propto \lambda \rho_v \left[\left(\frac{D(\rho_l - \rho_v)}{\rho_v} \right) (g\, a/g) \left(C_1 + \frac{C_2 \sigma g_c}{\mu U_m} \right) \right]^{1/2} \tag{16}$$

The assumption embodied in (14) is that the number of bubble columns times their area times the frequency of bubble emission remains constant. This is so because W_v has been regarded as proportional only to the variables ρ_v and U_m. Chang (*1*) has arrived at this result analytically, but there is only indirect experimental justification for the assumption. The indirect justification stems from the fact that it is well known that the area-frequency-number of columns product is important in determining the heat-transfer coefficient, h, in boiling (see for instance reference *17*), and three references (*10, 11, 12*) have shown that little difference in h exists owing to the imposition of up to 40 g acceleration on a boiling system.

U_m is proportional to $(q/A)_p$ which is relatively low at low values of a/g. Assume that at low a/g the value of U_m is low enough so that the term multiplied by C_2 in Equation (16) is large compared to constant C_1. Then, when property variations and C_1 in Equation (16) are neglected

$$(q/A)_p \propto \left[\frac{D(a/g)}{U_m} \right]^{1/2} \tag{17}$$

or, when the value of U_m from Equation (15) is substituted, one obtains

$$(q/A)_p \propto (D\, a/g)^{1/3} \tag{18}$$

It has been noted that the diameter of bubbles at break-off is inversely proportional to the square root of acceleration in nucleate boiling (*11, 12*). When it is assumed that the diameter D of the jet, which may be composed of several bubbles, is similarly effected by acceleration, (which would be entirely reasonable in terms of a force balance at the time that a group of bubbles leaves a surface) one obtains

$$D \propto (a/g)^{-0.5} \tag{19}$$

With Equations (18) and (19)

$$(q/A) \propto (a/g)^{0.5/3} = (a/g)^{0.167} \tag{20}$$

This is quite close to the behavior noted up to $a/g = 10$ in Figures 3, 4, and 7. With $a/g > 10$, it is assumed that the velocity U_m become slarge, so that the term containing $1/U_m$ in Equation (16) becomes small compared to C_1. This assumption is reasonable in view of statements by Chang (*1*) and others that surface tension effects become small at high convective velocities. In the present case, very high velocities result from the augmented buoyancy forces (*16*). The neglect of the surface tension term is further justified in view of the data shown in Figure 7, which indicate that curves for the different surface tensions tend to converge at high values of a/g. If the term involving σ and property variations with a/g is neglected Equation (16) yields

$$(q/A)_p \propto [D(a/g)]^{1/2} \tag{21}$$

or again with Equation (19)

$$(q/A)_p \propto (a/g)^{1/4} \tag{22}$$

which is almost the behavior for $a/g > 10$ in Figures 3, 4, and 7.

With Equation (16) it is also possible to explain tentatively the rapid increases of $(q/A)_p$ with (a/g) shown by heaters on which the vapor forms a long, flat wave before leaving the surface. Such waves of vapor, typically appear on that portion of cylindrical heaters toward which the acceleration is directed. The waves are formed as individual bubbles start to migrate around the heater and join with other vapor bubbles en route to the detaching side of the heater. Because of the geometry of these waves, surface tension effects are reduced.

It seems reasonable that when these waves appear, their length will be dictated largely by the extent and number of nuclation sites on the heater and not by the equality of surface tension and buoyancy forces which leads to Equation (19). Indeed, waves seen leaving the heaters were often almost as long as the active length of the heater. It may be assumed with some certainty that under this condition of operation, Equation (19) no longer holds, that surface tension effects are negligible, and that D in Equation (16) stands for the significant dimension of the wave which is nearly constant with acceleration. Since viscous, inertial, and gravity forces may still be important, the Reynolds number and the ratio of Reynolds to Froude number will be significant and Equation (16) may be used. If the group involving surface tension is regarded as small, Equation (21) again results, and if D is regarded as constant

$$(q/A)_p \propto (a/g)^{0.5} \tag{23}$$

Equation (10), which represents the behavior of semicylinders with the acceleration vector directed toward them, shows that the data tended toward the behavior predicted by Equation (23), but possibly some effects of surface tension still remained. The orientation for which Equation (10) holds is the one which gave rise to waves of vapor. No such waves originated on the halves of cylinders from which the acceleration was directed, and in these cases the peak heat flux was nearly proportional to acceleration to the one-quarter power.

The reduction of fluid surface tensions resulted in the data tending toward the behavior of Equation (23). The reduction in surface tension made the bubbles small and numerous, and it seems likely that no individual bubble columns left the heater, but that waves of vapor, formed by coalescence of the more numerous bubbles, swept off together. (No photographic evidence of this was gathered, however.) If this is the case, the same arguments used to derive Equation (23) apply and the equation should also hold for cases of very low surface tensions.

The arguments leading to Equation (23) have not been proven, but it is safe to say that reductions in surface ten-

sion and wave formation make the data tend toward the behavior predicted by the equation and away from the one-quarter power variation. It is noteworthy that the data of Gambill and Greene (*4*) show almost the same behavior as the present low surface tension tests. In experiments of Gambill and Greene, little surface tension effect would be present owing to the mode of operation (high convective velocity).

CONCLUSIONS

One may tentatively conclude from the foregoing that:

1. For narrow graphite flat plates and small cylindrical heaters in pure water, the peak heat flux varies with a/g to the 0.15 power for a/g values from somewhat less than unity to 10, provided that the accelerations are not directed toward the heaters. If $a/g > 10$, peak heat flux varies with a/g to about the 0.25 power.
2. Little difference was noted in the peak heat flux behavior owing to orientation of the acceleration vector except where the vector was wholly or partially directed toward a flat or cylindrical surface. For semicylinders, if the vector is directed normally toward the axis, the peak heat flux increases with a/g to powers as great as 0.38. For flat plates, the bubbles are held against the heater and the peak heat flux actually declines with a/g.
3. With reduced surface tension, peak heat flux increases with a/g to powers close to 0.50 if the accelerations are directed away from the surface.
4. Inclusion of viscous, inertial, buoyancy, and capillary forces leads to an equation explaining the variation of $(q/A)_p$ with a/g. Effects of these forces are not included in many existing analytic correlations for peak heat flux.

ACKNOWLEDGMENTS

The authors are extremely grateful for the generous support of this project afforded by the National Science Foundation. Mr. J. Wildy, Mr. A. Lord, and Mr. H. Epp were the extremely ingenious and tremendously conscientious technicians. Mr. Colin A. Heath provided excellent suggestions during the preparation of the paper.

NOTATION

a = acceleration, total, including centripetal plus local gravitational acceleration L/T^2
a_s = supplementary or Coriolis acceleration, L/T^2
C_1, C_2, C_3 = dimensionless constants
D = diameter of vapor jet rising through the liquid,, L
F = force per unit volume; F_r, in r direction; F_z, in z direction, F/L^3
g = local acceleration of gravity, L/T^2
g_c = constant of proportionality, $M\text{-}L/F\text{-}T^2$
P = pressure, F/L^2
$(q/A)_p$ = peak heat flux in nucleate pool boiling, $F\text{-}L/T\text{-}L^2$
r = coordinate of cylindrical jet (Figure 12) L; $\overline{r}$, normalized radius defined by (26), dimensionless
U, u = velocity of vapor in direction of jet axis, L/T. U_m, maximum velocity of jet before instability L/T; $\overline{U}$, normalized velocity defined by (26), dimensionless
V, v = velocity of vapor in radial direction with respect to jet, L/T, V_m, velocity of disturbance causing onset of instability, L/T; $\overline{V}$ normalized velocity defined by (26), dimensionless
W_v = maximum mass rate of vapor jet flow per unit area, M/L^2T
z = direction measured along axis of vapor jet and hence along radius of container, L. $\overline{z}$ normalized distance defined by (26), dimensionless

Greek Letters

α = angle of heater, measured from radial line (degrees) (Figure 6)
λ = latent heat of vaporization, $F\text{-}L/M$
μ = viscosity of vapor, $M/L\text{-}T$
μ_l = viscosity of liquid, $M/L\text{-}T$
ρ = density; ρ_l of liquid; ρ_v of vapor, M/L^3
σ = surface tension, F/L
ω = angular velocity, $1/T$

LITERATURE CITED

1. Chang, Y. P., *Trans. Am. Soc. Mech. Engrs.*, Series C, **85**, 89 (1963).
2. Zuber, N., M. Tribus, and J. W. Westwater, *Intern. Developments in Heat Transfer*, **2**, 230 (1961).
3. Borishanskii, V. M., *Soviet Phys. Tech. Phys.* (*Eng. Transl.*), **1**, No. 2, p. 438 (1956).
4. Gambill, W. R., and N. D. Greene, *Chem. Eng. Progr.*, **54**, 69 (1958).
5. ———, R. D. Bundy, and R. W. Wansbrough, Oak Ridge National Lab. *2911* (1960).
6. Costello, C. P., and J. M. Adams, *Intern. Developments in Heat Transfer*, **2**, 255 (1961).
7. Choi, N. Y., Ph.D. thesis, Mass. Inst. Technol., Cambridge, Mass. (1962).
8. Usiskin, C. M., and R. Siegel, *Trans. Am. Soc. Mech. Engrs.*, Series C, 83, 243 (1961).
9. Ivey, H. J., Paper submitted to the Inst. Mech. Engrs., London, England (April, 1962).
10. Merte, H., and J. A. Clark, *Trans. Am. Soc. Mech. Engrs.*, Series C, 83, 233 (1961).
11. Slember, R. J., Ph.D. thesis, Univ. Pittsburgh. Pittsburgh, Pa. (1961).
12. Costello, C. P., and W. E. Tuthill, *Chem. Eng. Progr. Symposium Ser. No. 32*, **57**, 189 (1961).
13. Bernath, L., *ibid., No. 30*, **56**, 95 (1959).
14. Adams, J. M., Ph.D. thesis, Univ. Washington, Seattle, Wash. (1962).
15. Timoshenko, S., and D. H. Young, "Engineering Mechanics," 3 ed., p. 472, McGraw-Hill, New York (1951).
16. Costello, C. P., J. M. Adams, and W. W. Clinton, *A.I.Ch.E. Journal*, **8**, No. 4, p. 569 (September, 1962).
17. Westwater, J. W., and R. F. Gaertner, *Chem. Eng. Progr.*, **55**, 58 (October, 1959).
18. Kline, S. J., "Approximation Theory Similitude and Dimensional Analysis," Chapter 4, to be published by McGraw-Hill, New York. Copies now available from Dr. S. J. Kline, Stanford University, Stanford, Calif.

Manuscript received November 7, 1962; revision received April 5, 1963; paper accepted April 5, 1963. Paper presented at A.I.Ch.E. Chicago meeting.

APPENDIX

Derivation of Pertinent Dimensionless Groups from the Navier-Stokes Equations

It is assumed that nucleate boiling continues until bubbles reach a limiting velocity, U_m, at which instability causes vapor to be washed back onto the heater surface (*1*).

Consider a cylindrical column of vapor or group of bubbles rising in a liquid which is flowing countercurrently (Figure 8). The vapor is flowing in the direction of the acceleration vector owing to buoyancy forces, and velocities are low enough so that compressibility effects are negligible. When simplified forms of the Navier-Stokes equations are written in cylindrical coordinates for the outside element of the vapor jet in steady flow

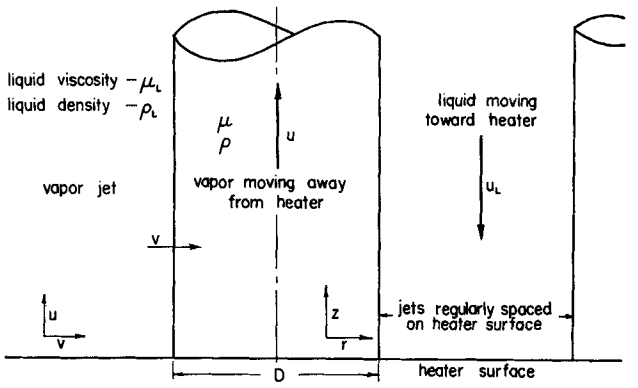

Fig. 8. Geometry of vapor jets or vapor bubbles for analysis in Appendix. System is two-dimensional with jets or bubbles forming approximately cylindrical surfaces.

$$\rho_v \left[V \frac{\partial U}{\partial r} + U \frac{\partial U}{\partial z} \right] = g_c F_z + \mu \left[\frac{\partial^2 U}{\partial z^2} + \frac{\partial^2 U}{\partial r^2} + \frac{1}{r} \frac{\partial U}{\partial r} \right] \tag{24}$$

$$\rho_v \left[V \frac{\partial V}{\partial r} + U \frac{\partial V}{\partial z} \right] = g_c F_r + \mu \left[\frac{\partial^2 V}{\partial r^2} + \frac{1}{r} \frac{\partial V}{\partial r} - \frac{V}{r^2} + \frac{\partial^2 V}{\partial z^2} \right] \tag{25}$$

F stands for force per unit volume and the rest of the nomenclature is defined on Figure 8. Pressure variation terms associated with the Navier-Stokes equations $\left(\frac{\partial P}{\partial r}, \frac{\partial P}{\partial z} \right)$ have been neglected.

When the Navier-Stokes equations are normalized and simplified boundary conditions are introduced

$$\overline{U} = \frac{U}{U_m} \qquad \overline{r} = \frac{r}{D}$$
$$\overline{V} = \frac{V}{V_m} \qquad \overline{z} = \frac{z}{D} \tag{26}$$

U_m is the maximum velocity of vapor as limited by jet instability. Since U_m is the largest velocity possible, the definition insures that $\overline{U}$ will be of order 1.

V_m is the maximum velocity of a disturbance across the jet. It is assumed that this velocity gives rise to the peak heat flux condition by propagating a disturbance which causes the jet to break down. Again $\overline{V}$ is of order 1.

The z direction body force is owing to buoyancy and that in the r direction is owing to surface tension. These may be phrased as

$$g_c F_z = (\rho_1 - \rho_v) a = (\rho_1 - \rho_v) g \left(\frac{a}{g} \right) \tag{27}$$

$$g_c F_r = -\frac{\sigma}{D^2} g_c \tag{28}$$

When these forces and the normalized variables, Equation (26), are substituted into Equations (24) and (25), and the equations multiplied by $\frac{D^2}{U_m \mu}$ one obtains

$$\frac{D \rho_v U_m}{\mu} \left(\frac{V_m}{U_m} \right) \overline{v} \frac{\partial \overline{U}}{\partial \overline{r}} + \left(\frac{D \rho_v U_m}{\mu} \right) \overline{u} \frac{\partial \overline{U}}{\partial \overline{z}} = \frac{D^2 (\rho_1 - \rho_v) g}{U_m \mu} \left(\frac{a}{g} \right) + \frac{\partial^2 \overline{U}}{\partial \overline{z}^2} + \frac{\partial^2 \overline{U}}{\partial \overline{r}^2} - \frac{1}{\overline{r}} \frac{\partial \overline{U}}{\partial \overline{r}} \tag{29}$$

$$\frac{D \rho_v U_m}{\mu} \left(\frac{V_m}{U_m} \right)^2 \overline{v} \frac{\partial \overline{V}}{\partial \overline{r}} + \frac{D \rho_v U_m}{\mu} \left(\frac{V_m}{U_m} \right) \frac{\partial \overline{V}}{\partial \overline{z}} =$$

$$\frac{-\sigma g_c}{U_m} + \left(\frac{V_m}{U_m} \right) \left[\frac{\partial^2 \overline{V}}{\partial \overline{r}^2} + \frac{\partial \overline{V}}{\partial \overline{r}\, \overline{r}} - \frac{\overline{V}}{\overline{r}^2} - \frac{\partial^2 \overline{V}}{\partial \overline{z}^2} \right] \tag{30}$$

The equation of continuity in cylindrical coordinates is

$$\frac{\partial U}{\partial z} + \frac{\partial V}{\partial r} + \frac{V}{r} = 0 \tag{30a}$$

If the equation is normalized with the variables in Equation (26)

$$\frac{U_m}{V_m} \frac{\partial \overline{U}}{\partial \overline{z}} + \frac{\partial \overline{V}}{\partial \overline{r}} + \frac{\overline{V}}{\overline{r}} = 0 \tag{30b}$$

Since all of the barred quantities are of order unity, U_m/V_m must also be of order unity. Thus groups with U_m/V_m will not differ appreciably from groups without this ratio, and the ratio may be neglected.

The requirements of approximation theory outlined by Kline (*18*) have all been fulfilled in the normalization employed above. Kline's treatment shows that if the requirements are fulfilled, the order of magnitude of the dimensionless groups which multiply barred quantities in Equation (30) reflects their relative importance in the final solution of differential Equation (30). That is, examination of the order of magnitude of the dimensionless groups should indicate which are of greatest significance in any solution of Equation (30). This is true because the dimensionless numbers should appear in the final solution in the same form and to the powers in which they appear in (30).

$\frac{D \rho_v U_m}{\mu}$, the Reynolds number, ratio of inertial to viscous forces, is of order 100 $U_m (a/g)^{-0.5}$ if it is assumed that D is of the order of one of the vapor slugs which leaves the surface, 0.02 ft. at $a/g > 1$. (This is not the individual bubble diameter, which is much smaller.) D is also considered inversely proportional to acceleration to the one-half power. (U_m is expressed in ft./sec. in the Reynolds group above.)

$\frac{D^2 (\rho_1 - \rho_v) g\, a/g}{U_m}$, the ratio of Reynolds to Froude number, is the ratio of gravitational to viscous forces. It is of the order $\frac{10^5}{U_m}$ if the comments above are considered in an evaluation of D. (U_m in ft/sec).

$\frac{\sigma g_c}{U_m \mu}$ is the ratio of Reynolds to Weber number; that is, ratio of cohesive to viscous forces. It is of the order $\frac{10^4}{U_m}$.* (U_m in ft/sec.)

Since these groups are large in comparison to the other terms of Equations (29) and (30) which are all of order one, it appears that these groups are the most significant ones included in a correlation of peak heat flux data based on hydrodynamic considerations. Other ratios of properties may enter (3) as well as parameters accounting for surface effects.

It is thought that the groups derived above contain the significant functions of a/g, and hence they are employed in Equation (12) in a manner such as to give the best fit to the data presented in this paper.

---

* The neglected term $\frac{\partial P}{\partial z}$ also may be analyzed for order of magnitude. If Equation (6) for $\frac{\partial P}{\partial z}$ is modified for the vapor phase and multiplied by $\frac{D^2}{U_m \mu}$ as was done to other terms in (24) and (25), the order of magnitude of the resulting term will be $\frac{30}{U_m}$. This is much smaller than the other terms involved in (29) and (30).